Energy balance of thermoelastic martensite transformation under stress

H. Pham, O. Maisonneuve, André Chrysochoos

Energy balance of thermoelastic martensite transformation under stress

A. Chrysochoos, H. Pham, O. Maisonneuve

Laboratoire de Mécanique et Génie Civil, URA CNRS 1214, Université Montpellier II, c.c. 081, Place Eugène Bataillon, F-34095 Montpellier Cedex 5, France

Abstract

Energy balances of pseudoelastic behaviour of a shape memory alloy are experimentally determined using IR techniques. In fact, these balances, established for Cu–Zn–Al alloy at constant room temperature and under quasi-static tensile conditions, allow us to study the relative importance of the intrinsic (mechanical) dissipation involved in austenite–martensite phase changes compared with thermomechancial couplings. An analysis of the experimental data shows that the thermoelastic austenite–martensite phase transition can be considered as a non-isothermal process involving no or little (hardly measureable) mechanical dissipation.

Assuming a non-dissipative phase transition, numerical simulations are done in the case of non-isothermal processes using two existing models. This numerical exercise gives mechanical, thermal and energetic responses that can be qualitatively compared with those obtained experimentally. These results evidence that an intrinsic dissipation is not necessary to describe the pseudoelastic behaviour. In general, this example emphasizes once again that thermal and mechanical analyses should be carried out jointly to characterize properties of materials.

1. Introduction

It is now well known that the pseudoelastic behaviour of shape memory alloys (SMAs) is due to austenite–martensite phase transitions. From a mechanical point of view these phase transitions give rise, under certain conditions, to hysteresis loops on the stress–strain curves of load–unload cycles at constant room temperature.

The literature dealing with the SMA phenomenology gives us several possible interpretations of this pseudoelastic hysteresis (e.g. Ortin and Planes, 1988; Van Humbeek, 1981; Wayman, 1983) which is related to internal energy variation of the material. First, the energy corresponding to hysteresis loops can be interpreted in terms of dissipated energy due to internal friction; second, in terms of stored energy associated with inter- and intragranular deformation incompatibilities; and third, as heat transfers with the surrounding induced by temperature variations due to the latent heat of phase change.

However, from a macroscopic point of view the pseudoelastic hysteresis seems to be only describable in the case of isothermal processes by taking into account dissipative phenomena (e.g. Frémond, 1987; Lexcellent and Licht, 1991).

In this paper, after a brief recall of the thermodynamic framework, a macroscopic analysis of the thermomechanical couplings associated with

pseudoelastic behaviour is presented. This analysis is based on tests performed with an experimental set-up using IR techniques. Quasi-static uniaxial pulsating tests have been done at constant room temperature on polycrystalline Cu–Zn–Al samples. The temperature variations of the sample are recorded through a numerization system. The processing of thermal data gives the amount of heat involved during the martensitic transformations. The main experimental observation leads us to consider the solid–solid phase change as a nondissipative (in the sense of the intrinsic dissipation) and anisothermal thermodynamic process.

To determine the influence of such a result on the mechanical predictions of classical models, numerical simulations are performed. This numerical exercise allows us to show that the observed temperature variations are sufficient to justify, qualitatively and quantitatively, the form and size of the mechanical hysteresis loops.

2. Thermodynamic framework

Classical concepts and results of the thermodynamics of irreversible processes are used (Boccara, 1968; Germain, 1973).

At each instant t the thermodynamic state of a homogeneous volume element is characterized by a set of $n+1$ state variables $(\alpha_0, \alpha_1, \ldots, \alpha_n)$. Let us take T $(T=\alpha_0)$ as the absolute temperature, ε $(\varepsilon=\alpha_1)$ as the strain tensor and α_j $(j=2, \ldots, n)$ as a set of $n-1$ internal variables completing the description of the thermodynamic state. The specific Helmholtz free energy is denoted by ψ and s symbolizes the specific entropy.

With this notation the Clausius–Duhem inequality that is deduced from the local form of the second principle of thermodynamics is written as

$$d=\sigma:\dot{\varepsilon}-\rho\frac{\partial\psi}{\partial\alpha_i}\dot{\alpha}_i-\frac{\boldsymbol{q}}{T}\,\mathbf{grad}\,T\geqslant 0,\ i=1,\ldots,n \quad (1)$$

where σ is the Cauchy stress tensor, ρ is the mass density, $\boldsymbol{q}$ is the heat influx vector and d is the dissipation. When d is equal to zero, the irreversible entropy production rate (d/T) is also equal to zero and the process is called reversible. Classically, the intrinsic dissipation d_1 (mechanical dissipation) is assumed to be positive and is given as

$$d_1=\sigma:\dot{\varepsilon}-\rho\frac{\partial\psi}{\partial\alpha_i}\dot{\alpha}_i\geqslant 0,\ i=1,\ldots,n \quad (2)$$

Under the experimental conditions of the tests presented here, it is shown (Chrysochoos, 1987) that the heat equation can be simplified as

$$\rho C_\alpha\dot{\theta}-k\Delta\theta=d_1+\rho T\frac{\partial^2\psi}{\partial T\partial\alpha_i}\dot{\alpha}_i=w'_{ch},\quad i=1,\ldots,n \quad (3)$$

where θ is the variation in temperature $(\theta=T-T_0$, with T_0 the equilibrium absolute temperature). The specific heat capacity C_α and the isotropic conduction tensor k are assumed to be constant. The term w'_{ch} symbolizes the volume heat sources that have been gathered in the second term of Eq. (3): we can find the intrinsic dissipation d_1 and the crossing terms corresponding to the thermomechanical couplings (thermoelastic effects, latent heat in the case of solid–solid phase transition, etc.).

3. Experimental results

3.1. Experimental arrangement and calibration

3.1.1. General description

The original feature of the experimental set-up is to record and use the temperature field of the sample surface to evaluate the amount of heat exchanged between the sample gauge length and the surroundings during mechanical tests. This set-up (Fig. 1) consists of a computerized uniaxial testing machine (**1**, **2**, **3**) and an IR thermography device (**5**, **6**, **7**). The latter is made of an IR camera (**5**), and display unit (**6**) and a numerization system (**7**) allowing the storage and processing of thermal pictures in a second microcomputer (**8**).

The numerization system was initially conceieved by J.C. Chezeaux and B. Nayroles (Nayroles et al., 1981) and then developed and improved by A. Chrysochoos and J.C. Dupré (Chrysochoos and Dupré, 1992). The pictures obtained are matrices of 256 lines by 180 columns

numerized on 12 bits. Moreover, the numerization system allows us to record at the beginning of each line of a thermal picture, by means of **4**, the corresponding load and deformation signals and four other electrical signals such as thermal level and thermal range characterizing the state of the camera.

Practically, the use of spatial numerical filtering (convolutive filters) reduces the noise of the video signal to temperature variations within 5×10^{-3} °C near room temperature.

The thermoregulation is carried out carefully. The test area must be completely closed. The air of the testing room is circulated using electric fans and the temperature controlled with two heat sources (air conditioner and fan heater).

3.1.2. Calibration of the video signal

A special warning target equipped with thermocouples has been realized to calibrate the variations (near room temperature) in the video signal. The response of the IR detector (MCT detector, liquid nitrogen cooled) is strongly non-linear even near thermal equilibrium. The calibration law has been approximated by a quadratic law (second-order approximation).

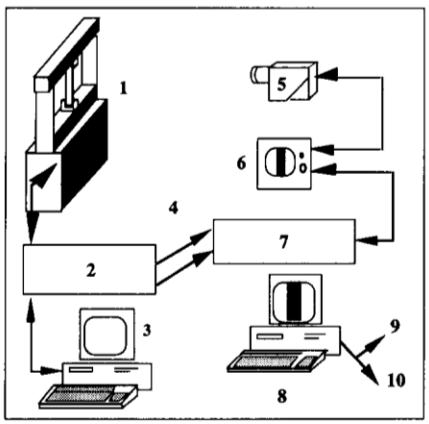

Fig. 1. Basic sketch of experimental set-up: **1**, uniaxial testing machine (100 kN); **2**, command unit; **3**, microcomputer 1 (loading parameters control, mechanical data storage and processing); **4**, transfer unit for load, stroke and extensometer signals; **5**, IR camera (InSb detector, liquid nitrogen cooled); **6**, display unit; **7**, numerization system of video signal (THERMAK); **8**, microcomputer 2 (storage, visualization and processing of thermal data); **9**, **10**, printer or plotter output.

Table 1
Thermomechanical properties of Cu–70.17Zn–25.63Al (wt.%) polycrystalline alloy

E (Young modulus)	24 GPa
ν (Poisson ratio)	0.33
λ_{th} (thermal expansion)	18×10^{-6} °C^{-1}
ρ (mass density)	7700 kg m^{-3}
C_x (specific heat)	393 J kg^{-1} °C^{-1}
k (thermal conductivity)	80 W m^{-1} °C^{-1}
L (specific latent heat)	7000 J kg^{-1}

Notice that the calibration can be performed in a dynamic way, i.e. it is not necessary to wait for thermal equilibrium, and therefore can be done frequently.

3.2. Material and experiment

Flat samples of a polycrystalline alloy (Cu–70.17Zn–25.63Al, wt.%) have been used. The transformation temperatures of this alloy are $M_s = 15$ °C, $M_f = 6$ °C, $A_s = 7$ °C and $A_f = 19.5$ °C. The slope of the transition line is around 2 MPa °C^{-1}; the thermoelastic constants of the material are gathered in Table 1.

To make sure of an initial austenite state, the samples are annealed at 850 °C for 10 min and then oil quenched for 1 h (Vacher, 1991). The storage temperature of samples is higher than 35 °C. Just before testing, a thin coat of black paint is laid down on the surface of each sample to improve its emissivity.

Two kinds of experiment have been performed: load–unload paths with increasing strain amplitude ($\varepsilon_{max} = 0.5\%, 1\%, 1.5\%$) and load–unload paths with constant strain amplitude ($\varepsilon_{max} = 1\%$). The tests are strain controlled during the loading and stress controlled during the unloading to avoid buckling phenomena. During the experiments the room temperature is held nearly constant at 30 °C (higher than A_f) and the absolute value of the strain rate is less than 1×10^{-3} s^{-1}.

In what follows, the interpretation of experimental data is done assuming quasi-static and homogeneous mechanical tests. Under these conditions, Figs. 2(a) and 2(b) show the mechanical responses for each kind of experiment. We can note that each load–unload path corresponds to a

hysteresis loop characterizing the pseudoelastic behaviour of the shape memory alloy.

3.3. Linking the temperature field to the heat sources

The temperature variations of the sample are obtained relative to a reference thermal picture. Fig. 3(a) represents the evolution with time of a thermoprofile in the direction of the loading axis during a test with increasing strain amplitude. In Fig. 3(b), thermoprofiles are plotted for several given instants. The length a represents the observation window size over which the energy balance

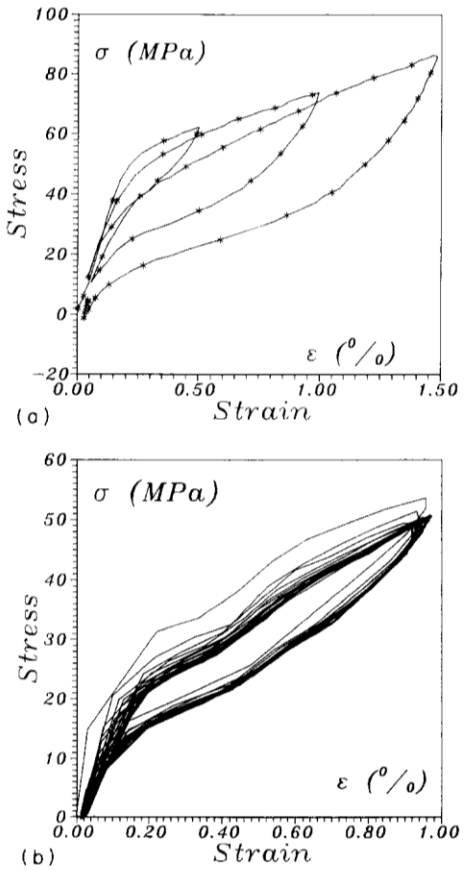

Fig. 2. (a) Mechanical response for load–unload cycles with increasing strain amplitude. (b) Mechanical response for load–unload cycles with constant strain amplitude: stabilization of hysteresis loops after several cycles.

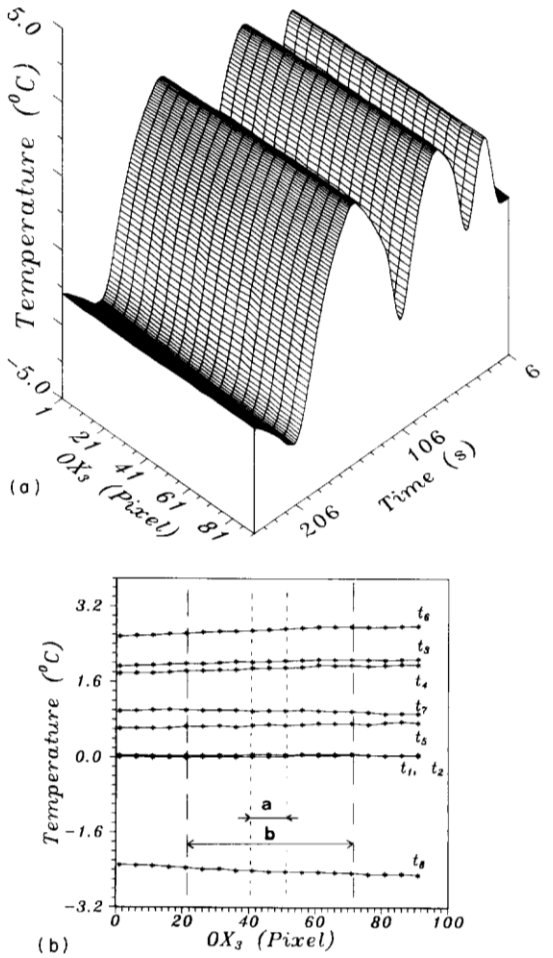

Fig. 3. (a) Evolution of thermoprofile parallel to loading axis plotted as a function of time. (b) Thermoprofiles extracted from (a) at eight different times (a, length of observation zone; b, gauge length of sample, 10 mm).

will be averaged and the length b corresponds to the gauge length of the sample. Looking at Fig. 3(b), we can easily assume that the temperature remains uniform at each instant t on this chosen observation window.

The evaluation of w'_{eh} is deduced from a numerical estimate of the time derivative and the temperature laplacian. From an experimental point of view the laplacian for good thermal conductors such as metallic alloys is quite difficult to evaluate directly near thermal equilibrium when the ther-

mal gradients are very small. Nevertheless, it is possible to determine the volume losses ($-k\Delta\theta/\rho C_\varepsilon$) by a numerical estimation of the differential operator. This estimation is based on a spatial filtering of data associated with finite differences and a validity control can be performed through numerical simulations (see Dupré (1991) for technical details).

In the particular case of quasi-static and homgeneous tests a linearization of the thermal losses is also possible. Then the local heat equation becomes

$$\rho C_\varepsilon\left(\frac{\partial\theta}{\partial t}+\frac{\theta}{\tau_{\text{th}}}\right)=w'_{\text{ch}} \tag{4}$$

where τ_{th} is a time constant characterizing the thermal losses. The energy amounts are calculated for the gauge volume ($V_0 = 150\ \text{mm}^3$):

$$W_{\text{ch}}(t)=V_0\int_{t_0}^{t} w'_{ch}(\tau)\,\mathrm{d}\tau \tag{5}$$

The evolutions of W_{ch}, θ and ε are plotted in Figs. 4(a) and 4(b).

3.4. Thermomechanical analysis

3.4.1. Experimental observations

From Figs. 4(a) and 4(b) the following remarks can be made.

Observation 1. The temperature variations can reach up to 7 °C. These variations are small compared with the absolute temperature but are not negligible in comparison with the size of the transition domain ($A_{\text{f}} - M_{\text{f}} \approx 13.5\ ^\circ\text{C}$).

Observation 2. The overall heat change W_{ch} between the sample and the surroundings is equal to zero at the end of each hysteresis loop within experimental accuracy.

3.4.2. Discussion

Observation 1 above leads us to consider the martensitic transformation under stress as a non-isothermal process. As a consequence, rather than assuming an isothermal process ($T = T_0$), we could adopt a linearized thermal approach ($\theta/T_0 \ll 1$). This first-order approximation will be called the small thermal perturbation hypothesis (STPH).

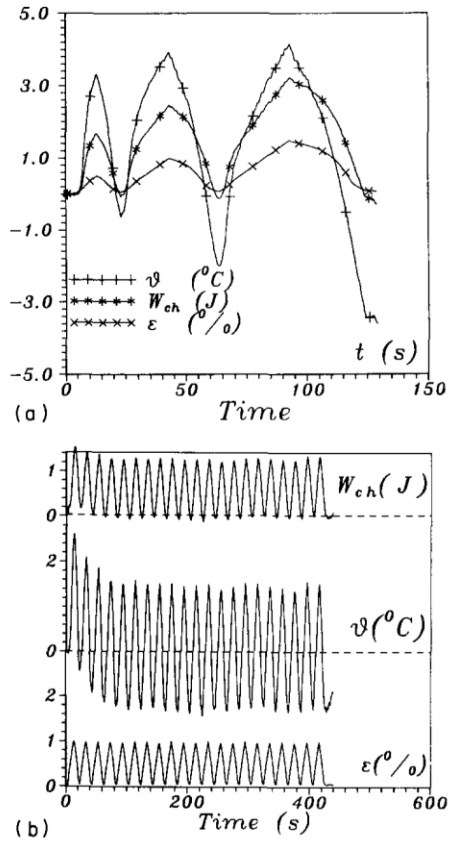

Fig. 4. (a) Load–unload cycles with increasing strain amplitude. Thermal response and evolution of heat W_{ch} (deduced from thermal data). This energy amount returns to zero at the end of each cycle. (b) Load–unload cycle with constant strain amplitude. Thermal response becomes periodic and symmetric after a few cycles. The heat W_{ch} returns to zero at the end of each hysteresis loop.

Then, to show the relative importance of dissipated energy compared with thermomechanical couplings, let us specify first the conditions required to associate a thermodynamic cycle with each hystersis loop, so that we get

$$\int_{\mathscr{C}} w'_{\text{ch}}(\tau)\,\mathrm{d}\tau = 0 \tag{6}$$

where $\mathscr{C}$ is the duration of the cycle. Second, let us show that the intrinsic dissipation d_1 is at most

of the same order of magnitude as θ/T_0 during such a thermodynamic cycle.

At the end of each hysteresis loop, we consider that the deformation returns to its initial value.

Moreover, the internal state of the material is again austenitic as soon as the stress is equal to zero for a temperature higher than A_f. Then we shall suppose a priori that the internal state variables α_j $(J = 2, \ldots, n)$, which represent here the volume proportions of the martensite twins, take their initial values again.

Because of heat diffusion, the temperature observations observed at the beginning and end of the pseudoelastic hysteresis can be different. However, the following two cases can occur.

(i) The temperatures T_i and T_f are the same (see the case of constant-amplitude pulsating tests after several load–unload cycles, Fig. 4(b)). In such a case each loop represents a thermodynamic cycle.

(ii) The temperature T_i and T_f are different but remain higher than A_f. Then the thermodynamic process can be fictitiously closed into a cycle by two thermoelastic transformations, the stress remaining equal to zero. These two transformations allow respectivley the passage from T_f to T_0 and from T_0 to T_i. Assuming a linear and isotropic thermoelastic behaviour, the supplementary amounts of heat evolved by these two transformations can then be written as

$$[W_{ch}]_f^0 + [W_{ch}]_0^i \approx -V_0[\lambda_{th}^2 T_0 E(T_i - T_f)] \tag{7}$$

where E is the Young modulus and λ_{th} is the thermal expansion.

For a maximum difference of 2 °C between T_i and T_f the value of the energy defined by Eq. (7) is around 2×10^{-3} J and corresponds to a strain amplitude less than 10^{-3}. These orders of magnitude are so small that they cannot be detected here.

Thus, associating a thermodynamic cycle with each hysteresis loop, which verifies Eq. (6), seems to agree with our observations. Now let us show that the intrinsic dissipation can be negligible during such a cycle.

For a thermodynamic cycle of duration $\mathscr{C}$ we than have

Table 2
Evolution of ratios R_T and R_M during tests with increasing strain amplitude

ε_{max} (%)	$W_{ch}(\mathscr{B})$ (10^{-3} J)	$V_0 \int_{\mathscr{B}} \lvert w'_{ch}(\tau)\rvert d\tau$ (10^{-3} J)	R_T (%)	$W_{ext}(\mathscr{B})$ (10^{-3} J)	R_M (%)
0.5	75	3585	2.1	6	18
1.0	140	5173	2.7	27	34
1.5	40	8010	0.5	55	43

$$\int_{\mathscr{C}} \rho \dot{s}\, d\tau = \int_{\mathscr{C}} \rho C_\varepsilon \frac{\dot{T}}{T} d\tau - \int_{\mathscr{C}} \rho \frac{\partial^2 \psi}{\partial T \partial \alpha_i} \dot{\alpha}_i\, d\tau = 0, \quad i = 1, \ldots, n \tag{8}$$

Since the first integral on the right-hand side of Eq. (8) must be equal to zero, the second one is also equal to zero. Taking into account the small variations in θ $(\theta/T_0 < 2\%)$, a linearized version of Eq. (3) integrated on the cycle yields

$$d_1 \approx 0 \tag{9}$$

This result is established for a polycrystalline alloy in the case of mechanical loadings at constant room temperature. It can be related to the one obtained by differential calorimetry on the same alloy during thermal loadings when the stress is equal to zero (Ortin, 1988). In every case it appears that if intrinsic dissipation takes place, it remains very small in comparison with the latent heat rate of phase change.

Table 2 describes, in the case of tests with increasing strain amplitude, the relative importance of dissipated energy. On one hand this relative importance can be evaluated by the ratio R_T defined in Eq. (10a). This ratio is equal to unity when the behaviour is exclusively dissipative (without any thermomechanical couplings) and zero when the behaviour is non-dissipative (under the SPTH). On the hand the hysteresis area can be characterized from a mechanical point of view by the ratio R_M defined in Eq. (10b). If the mechanical response is purely elastic (no hysteresis loop occurs), then the ratio R_M is equal to zero.

$$R_T = \frac{W_{ch}(\mathscr{B})}{V_0 \int_{\mathscr{B}} \lvert w'_{ch}(\tau)\rvert\, d\tau} \tag{10a}$$

$$R_M = \frac{W_{ext}(\mathscr{B})}{V_0 \int_{\mathscr{L}} \sigma : \dot{\varepsilon}\, d\tau} \tag{10b}$$

where $\mathscr{B}$ is the hysterisis loop duration whose load duration is $\mathscr{L}$. In Eq. (10b) the term $W_{ext}(\mathscr{B})$ is defined by

$$W_{ext}(\mathscr{B}) = V_0 \int_{\mathscr{B}} \sigma : \dot{\varepsilon}\, d\tau \tag{11}$$

and represents the deformation energy related to the hysteresis area.

First, we can note that the ratio R_T remains very small, which is in good agreement with a non-dissipative phase transformation hypothesis. Second, we can observe very small amounts of mechanical energy corresponding to the hysteresis area (less than 1×10^{-2} J) in comparison with the latent heats (greater than 1 J). Third, the "hysteresis energy" is not negligible against the mechanical energy provided by the testing machine to deform the sample ($R_M > 15\%$). Fig. 5 represents the energy balance associated with the pulsating test with increasing strain amplitude. We can observe that the amounts of heat evolved (latent heat) are considerably greater than the mechanical energy amounts.

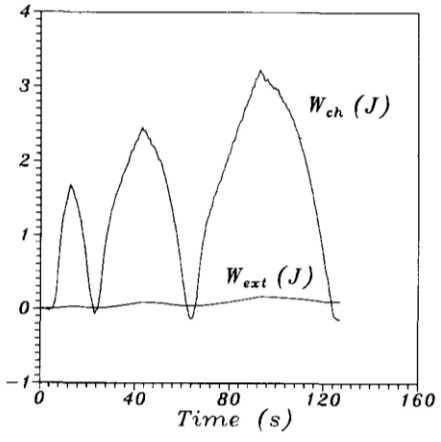

Fig. 5. Evolutions of evolved heat W_{ch} and deformation energy W_{ext} during a pulsating test. The difference in order of magnitude between the two energies can be observed.

4. Consequence on the modelling of the pseudoelastic behaviour

In this section the numerical predictions of two models are compared, assuming either an isothermal and dissipative phase transition (hypothesis H_1) or a non-isothermal and non-dissipative phase transition (hypothesis H_2).

Both models belong to the formalism of generalized standard materials (Halphen and Nguyen, 1975). The thermomechanical behaviour of materials is then described by two functions: a thermodynamic potential and a pseudopotential of dissipation. In most cases the specific Helmholtz free energy ψ is chosen. The dissipation potential ϕ is taken as a positive convex function depending on the rates of the state variables, $\dot{\alpha}_i$ ($i = 1, \ldots, n$), and is equal to zero at the origin. With these properties the Clausius–Duhem inequality is automatically verified.

For the sake of simplicity, both approaches will be applied in the monodimensional case (tensile test) and only one martensite twin will be considered. The state variables are T, ε and β, where β is the volume proportion of the martensite twin and verifies the inequality

$$0 \leqslant \beta \leqslant 1 \tag{12}$$

Of course, it is clear that the quantity $1 - \beta$ represents the volume proportion of austenite.

To take into account the inequality (12) in modelling, Frémond (1987) defined the free energy as the sum of the usual physical value and the indicator function $I_{\mathscr{T}}(.)$ of a convex set $\mathscr{T}$. If only one martensite twin is considered, then $\mathscr{T}$ is given as:

$$\mathscr{T} = \{\gamma \in \mathbb{R} | 0 \leqslant \gamma \leqslant 1\} \tag{13}$$

The function $I_{\mathscr{T}}(.)$ is convex and is defined by

$$I_{\mathscr{T}}(\beta) = \begin{cases} 0 & \text{if } \beta \in \mathscr{T} \\ \infty & \text{if } \beta \notin \mathscr{T} \end{cases} \tag{14}$$

For the mathematical treatment of Eq. (14) the basic convex analysis tools are necessary. It is recalled that the term $\partial f(x_0)$ denotes the subdifferential in x_0 of a convex function f defined on $\mathbb{R}^n$:

$$\partial f(x_0) = \{y \in \mathbb{R}^n | f(x) \geqslant f(x_0) + (x - x_0)y,\ \forall x \in \mathbb{R}^n\} \tag{15}$$

If f is a regular function in x_0, then $\partial f(x_0)$ is reduced to the gradient of f in x_0.

4.1. *Presentation of models*

4.1.1. *Model 1*

The first model is based on Frémond's (1987) approach. For the particular case in which only one martensite twin is taken into account, the expression of the specific free energy is given as

$$\rho\psi(T,\varepsilon,\beta)=\rho(1-\beta)\psi_a(T,\varepsilon)+\rho\beta\psi_m(T,\varepsilon)+I_{\mathscr{T}}(\beta) \tag{16}$$

The constant mass density ρ is assumed to be the same for all phases; the functions ψ_a and ψ_m are respectively the specific free energy of the austenite phase and the specific free energy of the martensite twin. Phase interactions are not taken into consideration.

If dissipation is exclusively due to the phase change, than the dissipation potential ϕ depends solely on the rate of β. Hence the behavioural constitutive equations are

$$\sigma=\rho(1-\beta)\frac{\partial\psi_a}{\partial\varepsilon}(T,\varepsilon)+\rho\beta\frac{\partial\psi_m}{\partial\varepsilon}(T,\varepsilon) \tag{17}$$

$$B^r\in\partial I_{\mathscr{T}}(\beta)+\partial\phi(\dot{\beta}) \tag{18}$$

$$B^r=-\rho[\psi_m(T,\varepsilon)-\psi_a(T,\varepsilon)] \tag{19}$$

If the behaviour is assumed non-dissipative, then Eq. (18) becomes

$$B^r\in\partial I_{\mathscr{T}}(\beta) \tag{20}$$

In this case the pseudoelastic hysteresis cannot be described as an isothermal process (Frémond, 1987).

To take into consideration phase interactions, Frémond suggested modifying the domain $\mathscr{T}$. Other trials can be seen in the literature (e.g. Müller and Xu, 1991) and it is the purpose of the next model.

4.1.2. *Model 2*

The second model is based on Lexcellent and Licht's (1991) approach. In this model, using the Legendre–Fenchel transform, the expression for the free energy is deduced from the specific enthalpy given by Patoor et al. (1987). The indicator function $I_{\mathscr{T}}(\beta)$ is introduced in the free energy form to improve the formal coherence of the model:

$$\rho\psi(t,\varepsilon,\beta)=\rho W_{elast}(\varepsilon-gR\beta,T)+\rho\beta W_{chem}(T)+\rho W_{int}(\beta)+I_{\mathscr{T}}(\beta) \tag{21}$$

The functions W_{elast}, W_{chem} and W_{int} represent respectively the thermoelastic energy, the chemical energy and the energy of interactions. The deformation due to the phase change is represented by $gR\beta$.

The dissipation potential ϕ depends solely on the rate of β; the constitutive equations then are

$$\sigma=\rho\frac{\partial W_{elast}}{\partial\varepsilon}(\varepsilon-gR\beta,T) \tag{22}$$

$$B^r\in\partial I_{\mathscr{T}}(\beta)+\partial\phi(\dot{\beta}) \tag{23}$$

$$B^r=gR\sigma-\rho W_{chem}(T)-\rho\frac{dW_{int}}{d\beta}(\beta) \tag{24}$$

In the case of a non-dissipative behaviour, Eq. (23) becomes

$$B^r\in\partial I_{\mathscr{T}}(\beta) \tag{25}$$

As in the former model, Eqs. (22), (24) and (25) cannot predict the pseudoelastic hysteresis if the temperature remains constant. In such a case, Eqs. (24) and (25) define a map-to-map relationship between σ and β (W_{int} being assumed strictly convex).

4.2. *Numerical simulations*

One-dimensional numerical simulations are performed using both preceding models. Load–unload cycles are considered and it is assumed that only one martensite twin is activated. Room temperature is constant and higher than A_f. For both models a viscous dissipation potential form is adopted to bring to light the incidence of hypothesis H_1:

$$\phi(\dot{\beta})=\frac{\eta}{2}\dot{\beta}^2 \tag{26}$$

where η is the viscosity coefficient.

4.2.1. Model 1

The free energy form defined in Section 4.1.1 can be decomposed into

$$\rho\psi_a(T, \varepsilon) = \tfrac{1}{2}E\varepsilon^2 - \rho\frac{L}{M_s}(T - M_s) - \rho C_\alpha T \log T \tag{27}$$

$$\rho\psi_m(T, \varepsilon) = \tfrac{1}{2}E\varepsilon^2 - \rho\alpha(T)\varepsilon - \rho C_\alpha T \log T \tag{28}$$

where $\alpha(T)$ is defined by

$$\alpha(T) = \begin{cases} -A(T - M_d) & \text{if } T \leqslant M_d \\ 0 & \text{otherwise} \end{cases} \tag{29}$$

Here L denotes the latent heat and M_d is the temperature above which no austenite–martensite transformation occurs ("martensite dead"). If a non-isothermal transformation is assumed, then the temperature equation evolution is determined by

$$W'_{ch} = \rho C_\alpha\left(\dot{\theta} + \frac{\theta}{\tau_{th}}\right) = d_1 + \rho T\beta A\dot{\varepsilon} + \rho T\left(A\varepsilon + \frac{L}{M_s}\right)\dot{\beta} \tag{30}$$

To obtain a qualitativey realistic hysteresis loop, the following coefficients have been chosen: $|\dot{\varepsilon}| = 10^{-4}\ s^{-1}$, $T_0 = 30\ °C$, $V_0 = 150\ mm^3$, $\rho = 7700\ Kg\ m^{-3}$, $E = 24\ GPa$, $C_\alpha = 393\ J\ kg^{-1}\ K^{-1}$, $M_s = 6\ °C$, $M_d = M_s + 65\ °C$, $L = 3000\ J\ kg^{-1}$, $A = 629.4\ J\ kg^{-1}\ K^{-1}$, $\tau_{th} = 60\ s$ if the process is regarded as nonisothermal, $\eta = 18 \times 10^6\ J\ m^{-3}\ s$ if the behaviour is assumed dissipative.

Figs. 6(a)–6(c) show the mechanical, thermal and energetic predictions for model 1. In each case computational exercises have been performed under hypothesis H_1 ($d_1 \neq 0$) and hypothesis H_2 ($d_1 = 0$). Fig. 6(d) shows the martensite proportion evolution.

4.2.2. Model 2

The various terms defined in Section 4.1.2. can be rewritten as

$$\rho W_{elast}(\varepsilon - g\beta, T) = \tfrac{1}{2}E(\varepsilon - g\beta)^2 - E\lambda_{th}(T - T_e)\varepsilon - \rho C_\alpha T \log T \tag{31}$$

$$\rho\beta W_{chem}(T) = \rho\beta(AT + B) \tag{32}$$

$$\rho W_{int}(\beta) = \rho D(\beta - 1)\beta \tag{33}$$

If a non-isothermal transformation is assumed, than the temperature equation evolution is determined by

$$W'_{ch} = \rho C_\alpha\left(\dot{\theta} + \frac{\theta}{\tau_{th}}\right) = d_1 - E\lambda_{th}T\dot{\varepsilon} + \rho AT\dot{\beta} \tag{34}$$

The coefficients taken in the simulations are as follows: $|\dot{\varepsilon}| = 10^{-4}\ s^{-1}$, $V_0 = 150\ mm^3$, $\rho = 7700\ kg\ m^{-3}$, $E = 24\ GPa$, $C_\alpha = 102\ J\ kg^{-1}\ K^{-1}$, $T_0 = 30\ °C$, $\lambda_{th} = 18 \times 10^{-6}\ K^{-1}$, $M_s = 6\ °C$, $M_f = 19\ °C$, $Rg = 0.013$, $A = 46.6\ J\ m^{-3}\ K^{-1}$, $B = -13611.4\ J\ m^{-3}$, $D = 40.6\ J\ m^{-3}$, $\tau_{th} = 20\ s$ if the process is regarded as non-isothermal, $\eta = 160 \times 10^6\ J\ m^{-3}\ s$ if the behaviour is assumed dissipative.

Figs. 7(a)–7(c) exhibit the mechanical, thermal and energetic predictions in the case of model 2. In Fig. 7(d) the kinetics of the phase change is plotted during a load–unload cycle.

4.2.3. Remarks

First, we can observe with both models that both hypotheses H_1 and H_2 give a hysteresis loop of the same order of magnitude. The ratios R_M are given in Table 3.

Second, we can note that even in the dissipative case (H_1) the ratio R_T can remain small. This is possible by using coefficients for the prediction of small dissipation (in comparison with the latent heat rate).

5 Concluding comments

The austenite–martensite phase change under stress at constant room temperature has been studied on Cu–Zn–Al samples from a thermomechanical point of view. The IR data corresponding to temperature variations of the material show that the transformations are non-isothermal processes. These variations remain small (around several degrees Celsius) in comparison with the absolute temperature. Nevertheless, they cannot be neglected compared with the transition domain size (around 10 °C). In a first-order approximation, associating a thermodynamic cycle with each

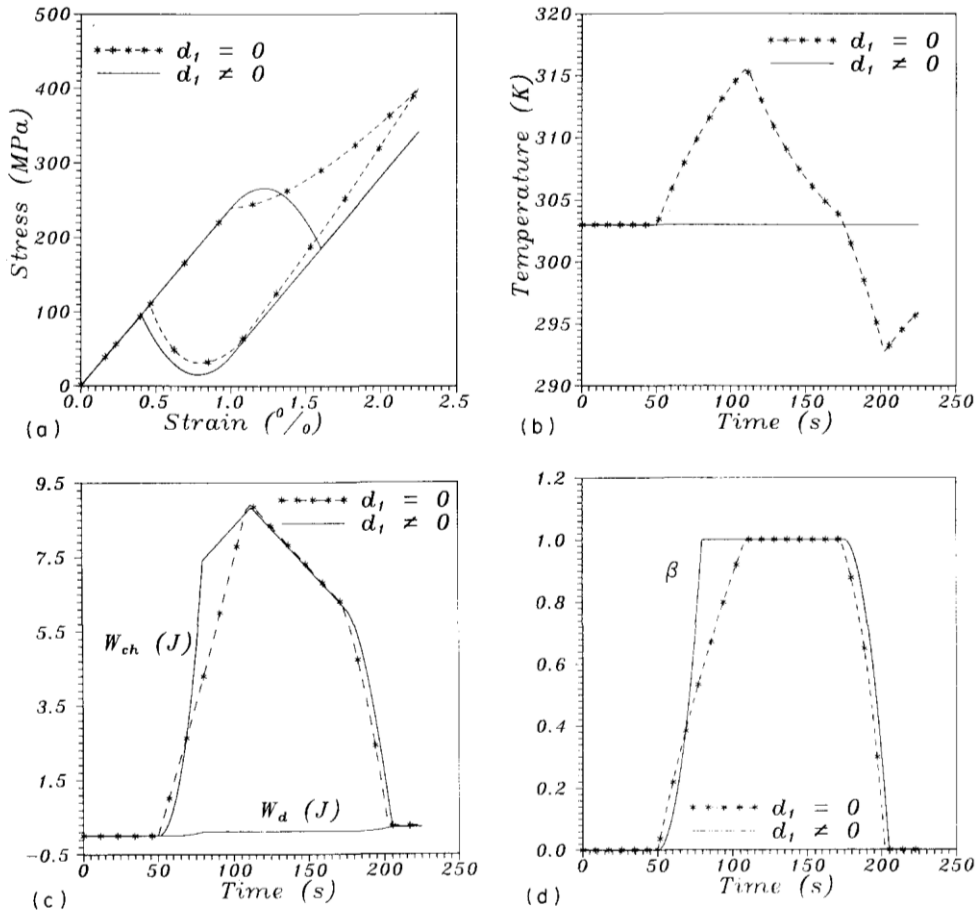

Fig. 6. (a) Mechanical predictions of model 1 under hypothesis H_1 ($d_1 \neq 0$) and hypothesis H_2 ($d_1 = 0$). (b) Temperature evolution under hypothesis H_1 and hypothesis H_2. Of course, with H_1 (full line) no temperature variation appears. (c) Energy balance (model 1). The thermoelastic couplings are only taken into account during the phase change. The term W_d stands for the energy dissipated within the equivalent volume V_0. Of course, with hypothesis H_2 (broken line) no dissipated energy can occur. (d) Evolution of martensite proportion β in case of model 1, i.e. kinetics of phase change during a load–unload cycle.

hysteresis loop yields a non-dissipative process. These results justify a non-isothermal and non-dissipative process hypothesis (H_2). The incidence of such a hypothesis has been underlined using two classical models. These models have been originally developed assuming a dissipative and

Table 3
Numerical simulations of ratios R_T and R_M

Model/ hypothesis	$\mathscr{W}_{ch}(\mathscr{B})$ (10^{-3} J)	$V_0 \int_{\mathscr{B}} \lvert w'_{ch}(\tau)\rvert d\tau$ (10^{-3} J)	R_T (%)	$\mathscr{W}_{ext}(\mathscr{B})$ (10^{-3} J)	R_M (%)	$\mathscr{W}_d(\mathscr{B})$ (10^{-3} J)
M_1/H_1	239	17439	1.4	239	36.4	239
M_1/H_2	262	17590	1.5	262	35.1	0
M_2/H_1	506	32450	1.6	505	27.4	506
M_2/H_2	529	32221	1.6	527	28.3	0

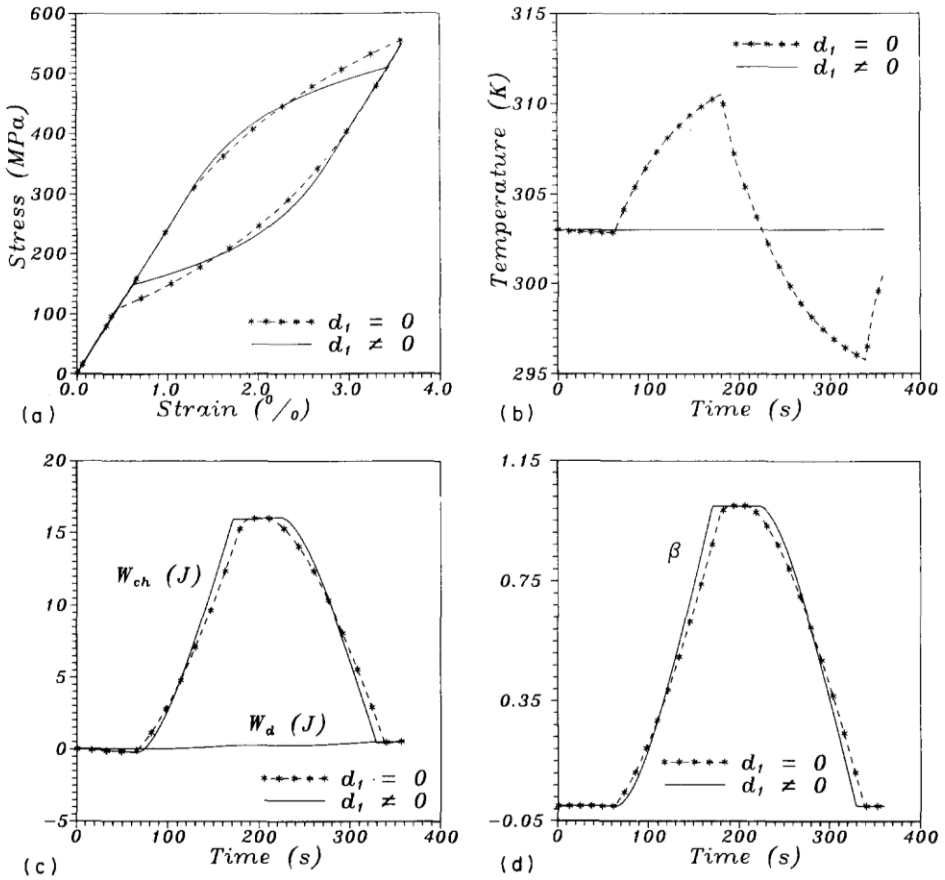

Fig. 7. (a) Mechanical Responses in the case of model 2. (b) Temperature evolution in the case of model 2. (c) Energy balance. The term W_d is the energy dissipated within the gauge volume V_0. (d) Evolution of martensite proportion that represents kinetics of phase change.

isothermal phase change (H_1). Numerical simulations show that significant hysteresis loops can be obtained by using indifferently either hypothesis H_1 or hypothesis H_2.

References

N. Boccara, Les Principes de la Thermodynamique, PUF, Coll. SUP, 1968.

A. Chrysochoos, Dissipation et blocage d'énergie lors d'un écrouissage en traction simple, Thesis, Montpellier, 1987.

A. Chrysochoos and J.C. Dupré, An infrared set-up for continuum thermomechanics, Proc. Colloq. QIRT, Eurotherm Seminar 27, Européennes thermiques et Industries, 1992.

J.C. Dupré, Traitement et analyse d'images pour la mesure des grandeurs cinématiques, (. . .), et pour l'étude de couplage thermomécaniques, Thesis, Poitiers, 1991.

M. Frémond, Matériaux à mémoire de forme, C.R. Acad. Sci., Sér. 2, 7 (1987) 239–245.

P. Germain, Cours de Mécanique des Milieux Continus, Tome 1, Masson, Paris, 1973, pp. 139–161.

B. Halphen and Q.S. Nguyen, Sur les matériaux standard généralisés, J. Méc. 14(1) (1975).

C. Lexcellent and C. Licht, Some remarks on the modelling of the thermomechanical behaviour of shape memory alloys, J. Phys. (Paris) IV, Colloq. C4, 1 (1991) 35–39.

I. Müller and H. Xu, On the pseudoelastic hysteresis, Acta. Metall. Mater. 39(3) (1991) 263–271.

B. Nayroles, R. Bouc, H. Caumon and J.C. Chezeaux, Thermograpie infrarouge et mécanique et structures, Int. J. Eng. Sci. (1981) 929–947.

J. Ortin and A. Planes, Thermodynamic analysis of thermal measurements in thermoelastic martensitic transformations, Acta. Metall. 36(8) (1988) 1873–1889.

J. Ortin, Thermodynamics of the martensitic transformation, in Technologie et Mise en Oeuvre des Alliages à Mémoire de

Forme, Cours Europeen COMETT II, La Ciotat, 1991, Chap. VI.

E. Patoor, A. Eberhart and M. Berveiller, Potentiel pseudoélastique et plasticité de transformation martensitique dans les mono et polycristaux métalliques, Acta Metall. 38 (1987) 2779–2789.

P. Vacher, Etude de comportement pseudoélastique d'alliages à mémoire de forme Cu–Zu–Al polycristallins, Thesis, Besançon, 1991.

J. Van Humbeek, The influence of strain-rate, amplitude and temperature on the hysteresis of a pseudoelastic Cu–Zn–Al single crystal, J. Phys. (Paris), Colloq. C5, 42(10) (1981) 1007–1011.

C.M. Wayman, Phase transitions, nondiffusive, in R.W. Cahn and P. Haasen (eds.), Physical Metallurgy, Part II, Elsevier, Amsterdam, 1983, pp. 1031-1047.

Appendix: Main nomenclature

A_f	"austenite finish"
A_s	"austenite start"
$\mathscr{B}$	hysteresis loop duration
$\mathscr{C}$	duration of thermodynamic cycle
$C\alpha$	specific heat capacity
d	dissipation
d_1	intrinsic dissipation
E	Young modulus
$\partial f(x_0)$	subdifferential in x_0 of convex function f
$I_{\mathscr{T}}(.)$	indicator function of convex set $\mathscr{T}$
k	isotropic conduction tensor
L	latent heat
$\mathscr{L}$	loading path duration
M_d	"martensite dead"
M_f	"martensite finish"
M_s	"martensite start"
$\boldsymbol{q}$	heat influx vector
s	specific entropy
t	time
T	absolute temperature
T_f	temperature at end of pseudoelastic hysteresis
T_i	temperature at beginning of pseudoelastic hysteresis
T_0	equilibrium absolute temperature
V_0	gauge volume of sample
w'_{ch}	volume heat sources
W_{ch}	amount of heat evolved
W_{chem}	chemical energy
W_{elast}	thermoelastic energy
$W_{ext}(\mathscr{B})$	mechanical energy or deformation energy related to hysteresis area
W_{int}	energy of interactions

Greek letters

α_l	state variables ($l = 0, \ldots, n$)
β	volume proportion of martensite twin
ε	strain tensor
η	viscosity coefficient
θ	variation in temperature
λ_{th}	thermal expansion
ρ	mass density
σ	Cauchy stress tensor
τ_{th}	time constant characterizing thermal losses
ϕ	pseudopotential of dissipation
ψ	specific Helmholtz free energy
ψ_a	specific free energy of austenite phase
ψ_m	specific free energy of martensite twin